Original Article

MOLECULAR METABOLISM

SORLA mediates endocytic uptake of proIAPP and protects against islet amyloid deposition

Alexis Z.L. Shih [1,2,*], **Yi-Chun Chen** [3,4,5], **Thilo Speckmann** [6,7], **Esben Søndergaard** [8], **Annette Schürmann** [6,7], **C. Bruce Verchere** [3,4,5], **Thomas E. Willnow** [1,2,9,**]

ABSTRACT

Objective: Sorting-related receptor with type A repeats (SORLA) is a neuronal sorting receptor that prevents accumulation of amyloid-beta peptides, the main constituent of senile plaques in Alzheimer disease. Recent transcriptomic studies show that SORLA transcripts are also found in beta cells of pancreatic islets, yet the role of SORLA in islets is unknown. Based on its protective role in reducing the amyloid burden in the brain, we hypothesized that SORLA has a similar function in the pancreas via regulation of amyloid formation from islet amyloid polypeptide (IAPP).

Methods: We generated human IAPP transgenic mice lacking SORLA (hIAPP:SORLA KO) to assess the consequences of receptor deficiency for islet histopathology and function *in vivo*. Using both primary islet cells and cell lines, we further investigated the molecular mechanisms whereby SORLA controls the cellular metabolism and accumulation of IAPP.

Results: Loss of SORLA activity in hIAPP:SORLA KO resulted in a significant increase in islet amyloid deposits and associated islet cell death compared to hIAPP:SORLA WT animals. Aggravated islet amyloid deposition was observed in mice fed a normal chow diet, not requiring high-fat diet feeding typically needed to induce islet amyloidosis in mouse models. *In vitro* studies showed that SORLA binds to and mediates the endocytic uptake of proIAPP, but not mature IAPP, delivering the propeptide to an endolysosomal fate.

Conclusions: SORLA functions as a proIAPP-specific clearance receptor, protecting against islet amyloid deposition and associated cell death caused by IAPP.

Keywords Beta cell; Endocytosis; IAPP; Islet amyloid; SORLA; VPS10P domain receptor

1. INTRODUCTION

Islet amyloid polypeptide (IAPP or amylin) is a peptide hormone secreted together with insulin by beta cells in the pancreatic islets of Langerhans. IAPP is synthesized as a 67 amino acid precursor ($proIAPP_{1-67}$) with two propeptide regions extended at its N- and C-terminus. The majority of $proIAPP_{1-67}$ and its partially processed intermediate $proIAPP_{1-48}$ are further processed and modified in secretory granules to yield the 37 amino acid mature IAPP [1,2]. IAPP contributes to energy homeostasis through mediating satiety, delaying gastric emptying, and modulating insulin secretion [3,4]. Human IAPP (hIAPP) is amyloidogenic and susceptible to aggregation into toxic oligomers and insoluble islet amyloid, a pathological feature of type 2 diabetes [5,6]. Impaired processing, overproduction, or impaired catabolism of IAPP may promote such amyloid deposition in the islet [7,8]. However, the regulation of IAPP production and turnover, which underlies islet amyloid formation, remains incompletely understood.

Similar to type 2 diabetes, accumulation of amyloid plaques is a pathological hallmark in Alzheimer disease (AD) [9]. The amyloidogenic agent in AD is amyloid-beta peptide (Aβ), a proteolytic product of the amyloid precursor protein (APP). Accumulation of Aβ in the brain is controlled by SORLA (sorting protein-related receptor containing LDLR class A repeats), a type I transmembrane receptor and major AD risk gene [10–12]. SORLA reduces overall Aβ burden via two mechanisms. Acting as an intracellular sorting receptor for APP, it moves the precursor from endosomal compartments to the Golgi to prevent proteolytic breakdown to Aβ in endosomes [10,13]. In addition, it sorts newly produced Aβ to lysosomes for catabolism, further reducing Aβ build-up in the brain parenchyma [14,15]. In line with a central role for SORLA in brain amyloidosis, genetic variants in its gene, *SORL1*, have been associated with sporadic [11,12] and familial [16] forms of AD.

[1]Max-Delbrück-Center for Molecular Medicine, Berlin, Germany [2]Charité — Universitätsmedizin Berlin, Corporate Member of Freie Universität Berlin and Humboldt-Universität zu Berlin, Berlin, Germany [3]BC Children's Hospital Research Institute and Centre for Molecular Medicine and Therapeutics, Vancouver, BC, Canada [4]Department of Pathology & Laboratory Medicine, University of British Columbia, Vancouver, BC, Canada [5]Department of Surgery, University of British Columbia, Vancouver, BC, Canada [6]Department of Experimental Diabetology, German Institute of Human Nutrition Potsdam-Rehbruecke (DIfE), Nuthetal, Germany [7]German Center for Diabetes Research (DZD), München-Neuherberg, Germany [8]Steno Diabetes Center Aarhus, Aarhus University Hospital, Aarhus, Denmark [9]Department of Biomedicine, Aarhus University, Aarhus, Denmark

*Corresponding author. Max-Delbrück-Center for Molecular Medicine, Robert-Rössle-Str. 10, D-13125 Berlin, Germany. E-mail: Alexis.Shih@mdc-berlin.de (A.Z.L. Shih).

**Corresponding author. Max-Delbrück-Center for Molecular Medicine, Robert-Rössle-Str. 10, D-13125 Berlin, Germany. E-mail: willnow@mdc-berlin.de (T.E. Willnow).

Received June 7, 2022 • Revision received July 27, 2022 • Accepted August 25, 2022 • Available online 30 August 2022

https://doi.org/10.1016/j.molmet.2022.101585

Abbreviations

Aβ	Amyloid-beta peptide
AD	Alzheimer disease
APP	Amyloid precursor protein
CPE	Carboxypeptidase E
GSIS	Glucose-stimulated insulin secretion
GTT	Glucose tolerance test
HFD	High-fat diet
hIAPP	Human islet amyloid polypeptide
IP	Intraperitoneal
KO	Knockout
ND	Normal diet
PAM	Peptidyl-glycine alpha-amidating monooxygenase
PC	Prohormone convertase
SORLA	Sorting protein-related receptor containing LDLR class A repeats
ThioS	Thioflavin S
VPS10P	Vacuolar protein sorting 10 protein
WT	Wildtype

On top of the relevance of SORLA for amyloidogenic processes in neurons, recent single-cell RNA sequencing analyses of human and mouse islets uncovered SORLA expression in pancreatic beta cells [17–19]. Because SORLA binds to a broad range of ligands [20], we hypothesized that this receptor may play a role in beta cell physiology; specifically, in regulating IAPP handling and islet amyloid formation. In this study, we tested if and how SORLA controls IAPP trafficking and processing, islet amyloid deposition, and glucose homeostasis. We examined the expression and subcellular localization of SORLA in islet beta cells and its interaction with pro- and mature forms of IAPP. Furthermore, we investigated the consequences of receptor deficiency for islet amyloid formation, beta cell function, and overall metabolic characteristics in mice expressing hIAPP, an animal model of islet amyloid deposition.

2. MATERIALS AND METHODS

2.1. Animal studies

Human IAPP transgenic (FVB/N-Tg(Ins2-IAPP)RHFSoel/J) mice were purchased from the Jackson Laboratory (#08232). Global SORLA knockout mice (*Sorl1*$^{-/-}$) on a C57BL/6J background were generated previously [10]. SORLA WT and KO mice expressing *hIAPP* transgene, as well as hIAPP-null littermates, were generated by crossing hIAPP transgenic males with *Sorl1*$^{+/+}$ or *Sorl1*$^{-/-}$ females, respectively. Since islet amyloid deposition is primarily observed in male hIAPP transgenic mice and rarely found in females [21], all experiments were conducted in male mice. Animals were housed in a facility with controlled environment, 12 h light/dark cycle, and fed a normal chow diet (4.5% crude fat) or a HFD (60% crude fat; #E15741-34; Ssniff, Germany). All animal experiments were performed according to protocols approved by the Berlin State Office for Health and Social Affairs (LAGESO, Berlin, Germany).

2.2. Intraperitoneal glucose tolerance test (IPGTT)

Prior to IPGTT, mice were fasted for 16 h (17:00—09:00). The next morning, mice were weighed and fasting blood glucose was measured in blood collected from the tail tip. For ND-fed mice, a glucose dose of 2.0 g/kg body weight was administered, while a lower glucose dose of 0.75 g/kg body weight was administered to HFD-fed mice to ensure that all glucose measurements fall within the detection range of the glucometer throughout the experiment. Blood glucose was measured at regular intervals from the tail tip.

2.3. Glucose-stimulated insulin secretion (GSIS) *in vivo*

Prior to *in vivo* GSIS, mice were fasted for 16 h (17:00—09:00). The next morning, mice were weighed and 100 μl of fasted blood was collected from the submandibular vein into EDTA-treated blood collection tube. For both ND- and HFD-fed mice, a glucose dose of 2.0 g/kg body weight was administered intraperitoneally. Insulin release was measured in blood collected from the other submandibular vein 30 min after glucose stimulation. Plasma was separated by centrifugation at 1500 x g for 10 min at 4 °C, and stored at −80 °C until further measurement by ELISA.

2.4. Islet isolation, dispersion and culture

Animals were sacrificed by cervical dislocation and the pancreas perfused with 2 ml of 900 U/ml collagenase (Sigma Aldrich, USA) in HBSS (Life Technologies, USA). After surgical removal of the pancreas, it was digested in 2 ml of collagenase solution at 37 °C for 13 min, followed by manual shaking for 60—90 s, two rounds of washing, and passing through a 70 μm filter. Islets were hand-picked and cultured in RPMI 1640 (PAN-Biotech, Germany) supplemented with 2 mM L-Glutamine, 100 U/ml penicillin, 100 mg/ml streptomycin, and 10% FBS (Gibco 10270-106). Islets were recovered overnight prior to secretion assays or dispersion. For subcellular localization studies, islets were dispersed into single cells by pipetting in 0.05% trypsin—EDTA (Gibco, USA) solution for 1 min, seeded onto uncoated glass coverslips, and cultured for six days prior to fixation.

2.5. Staining of tissues or cells for confocal microscopy

Mouse pancreata were harvested and fixed in 4% (wt/vol) paraformaldehyde overnight at 4 °C, subjected to a sucrose gradient with stepwise increase from 15% to 30% (wt/vol), and frozen at −80 °C in cryomolds containing OCT compound. Tissue sections (10 μm) were rehydrated in 0.3% Triton X-100 in PBS-T for 15 min, followed by antigen retrieval in 10 mM citrate buffer with 0.05% Tween-20 (pH 6.0) at 95 °C for 10 min. Human pancreas biopsies from three anonymized, healthy individuals were provided as paraffin-embedded sections by Assoc. Prof. Søndergaard (Steno Diabetes Center Aarhus). The human pancreas biopsies were obtained from two women undergoing surgery for endometrial cancer and from one man with resection of pancreas without any signs of malignancy or other disease. For dispersed mouse islet cells, cells were fixed in 4% (wt/vol) paraformaldehyde for 10 min at room temperature, then permeabilized in 0.3% Triton X-100 with 0.1% BSA in PBS-T (pH 7.4) for 10 min at room temperature. Both pancreatic tissues and islet cells were blocked in 3% BSA in PBS-T overnight at 4 °C, followed by sequential incubation in primary and secondary antibodies (Suppl. Table 1) for 2 and 1 h, respectively, at room temperature. Nuclei were visualized via DAPI staining. Images from a single z-plane were acquired using a Zeiss LSM 700 confocal microscope (10X objective for tissue samples; 63X objective for dispersed islet cells).

Amyloid staining: Islet amyloid was assessed based on thioflavin S (Sigma-Aldrich, USA) staining, as previously described [8]. Islet amyloid prevalence was quantified as the percentage of islets containing amyloid. Islet amyloid severity was quantified as percentage of ThioS-positive area over total islet area. Morphological

analyses were performed in CellProfiler (Cambridge, MA, USA). Both islet amyloid prevalence and severity were assessed based on the mean value of 22–30 islets per mouse.

TUNEL staining: Cell death was measured via terminal deoxynucleotidyl transferase dUTP nick end labeling (TUNEL) staining according to manufacturer instructions (Roche Applied Science, Germany). The percentage of TUNEL positive islet cells per mouse was determined as the mean of 22 to 30 islets, with an average of 259 ± 16 cells analyzed per islet.

Proximity ligation assay (PLA): PLA was performed on dispersed islet cells to assess close interaction (<40 nm) between endogenous SORLA and mouse IAPP (Peninsula Laboratories T-4145) or human IAPP (Peninsula Laboratories T-4149) in beta cells. The experiment was performed according to manufacturer's protocol (Sigma-Aldrich, USA). Beta cells and early endosomes were identified through immunostaining for insulin and Rab4, respectively.

2.6. Islet perifusion

The assay was performed using a PERI 4.2 machine (Biorep Technologies, USA). Groups of 30 islets were continuously perifused with KRBH buffer (129 mM NaCl, 4.8 mM KCl, 1.2 mM $MgSO_4$, 1.2 mM KH_2PO_4, 5 mM $NaHCO_3$, 2.5 mM $CaCl_2$, 10 mM HEPES and 0.25% BSA, at pH 7.4) with the indicated glucose concentration at a flow rate of 100 μl/min. Initially, islets were equilibrated in 11 mM glucose KRBH for 60 min (flow-through discarded), followed by sequential incubation (flow-through collected in 96-well plate) with 11 mM glucose (18 min), 1.67 mM glucose (60 min), 16.7 mM glucose (34 min), 1.67 mM glucose (30 min), and 30 mM KCl in 1.67 mM glucose KRBH (10 min). At the end of the assay, islets were retrieved and lysed in TE buffer (10 mM Tris–HCl, 1 mM EDTA and 1% Triton X-100) to measure DNA content (Quant-iT Picogreen DNA kit, Thermo Fisher Scientific, USA). Insulin levels were measured by ELISA and normalized to DNA content.

2.7. Acid ethanol extraction of insulin content in pancreas and islets

Total pancreas was excised, weighed, and placed in 5 ml of ice-cold acid ethanol solution (0.18 M HCl in 70% ethanol). Pancreatic tissues were mechanically homogenized and incubated in acid ethanol at 4 °C overnight. For insulin extraction from islets, 30 islets per pancreas sample were incubated in 30 μl of ice-cold acid ethanol and vortexed for 1 min. The homogenate was incubated on ice for 3 h with additional vortex every 30 min. The supernatants of pancreas and islet homogenates were collected by centrifugation at 2000 rpm for 15 min at 4 °C and stored at −80 °C until determination of insulin content by ELISA. The pancreatic insulin content was normalized to total pancreas weight, while islet insulin content was normalized to protein concentration as determined by bicinchoninic acid assay.

2.8. ELISAs

Insulin was measured using the Ultra Sensitive Mouse Insulin ELISA kit (Crystal Chem, USA). Human $proIAPP_{1-48}$ and mature IAPP were measured via an in-house ELISA as described [22].

2.9. Microscale thermophoresis (MST)

Mouse sequence of $proIAPP_{1-70}$, $proIAPP_{1-51}$ and mature amidated IAPP peptides (NCBI Reference Sequence: NP_034621) were synthesized commercially (Biosyntan, Germany). Peptides were dissolved in PBS and stored at −80 °C prior to binding assays. Recombinant His-tagged SORLA ectodomain (including residue 728-1526) was previously purified [10]. For microscale thermophoresis (MST), SORLA ectodomain was fluorescently labeled using the Protein Labeling Kit RED-NHS (NanoTemper Technologies, Germany). Concentrations of the target molecule (labeled SORLA ectodomain in PBS with 0.05% Tween 20, pH 7.4) was kept constant (3 nM), while the concentration of the non-labeled binding ligand (IAPP peptides) was serially titrated from 7.6 nM to 250 μM. K_d was derived using MO.Affinity Analysis software version 2.3 (NanoTemper Technologies, Germany).

2.10. Cell culture

Neuroblastoma SH-SY5Y cells (ATCC CRL-2266) were cultured in DMEM/F12 media (Gibco, USA) supplemented with 10% FBS, 1% NEAA, 100 U/ml penicillin and 100 mg/ml streptomycin. SH-SY5Y cells stably overexpressing SORLA were previously generated [15] and maintained in the presence of 90 μg/ml zeocin (Invitrogen, USA). Cells were routinely tested for mycoplasma infection.

2.11. IAPP peptide uptake assay

Synthetic mouse (pro)IAPP peptides were the same as described above. Synthetic human $A\beta_{1-40}$ peptides were purchased from Bachem, Germany (#4095737). SH-SY5Y parental cells and SH-SY5Y cells stably overexpressing SORLA were seeded onto uncoated glass coverslips one day prior to the peptide uptake assay. Cells were incubated in serum-free medium for 30 min prior to treatment with 20 μM (pro)IAPP for 30 min. Simultaneous treatment with 100 μM dynasore (Cayman Chemical, USA) was used to examine the role of clathrin-mediated endocytosis. Cells were fixed in 4% (wt/vol) paraformaldehyde and immunofluorescence staining was performed to visualize internalized peptides, SORLA, and subcellular organelles. Lysosomes were labeled by preincubating cells with 500 nM LysoTracker Deep Red (Thermo Fisher Scientific, USA) in normal growth media for 1 h prior to the uptake assay.

2.12. Statistical analysis

Statistical analyses were performed using GraphPad Prism 6.0 (GraphPad Software, USA). Normal distribution of data was tested with the D'Agostino-Pearson normality test. Data with sample size too small for normality test ($n < 8$) were analyzed by unpaired t-test. Comparisons of results between groups were analyzed using Student's t-test, one-way or two-way ANOVA. Data are presented as mean ± SEM.

3. RESULTS

3.1. SORLA is expressed in islet beta cells

First, we validated existing transcriptome data on SORLA expression in islets [17–19] by immunohistology on mouse and human pancreatic sections. In mouse islets, SORLA was mainly expressed in insulin-producing beta cells, but to some extent also in glucagon-producing alpha cells, somatostatin-producing delta cells and pancreatic polypeptide (PPY)-producing PP cells (Figure 1A). Expression of SORLA was lost in islets of mice carrying a targeted global disruption of *Sorl1*, hereinafter referred to as SORLA knockout (KO) (Figure 1B) [10]. In human islets, SORLA was predominantly expressed in beta cells and not found in alpha cells (Figure 1C). Overall, these data confirm SORLA expression in both murine and human beta cells.

3.2. Loss of SORLA increases islet amyloid prevalence and severity *in vivo*

To study the impact of SORLA activity on islet amyloid formation, we crossed SORLA KO mice (on a C57BL/6J background) with a

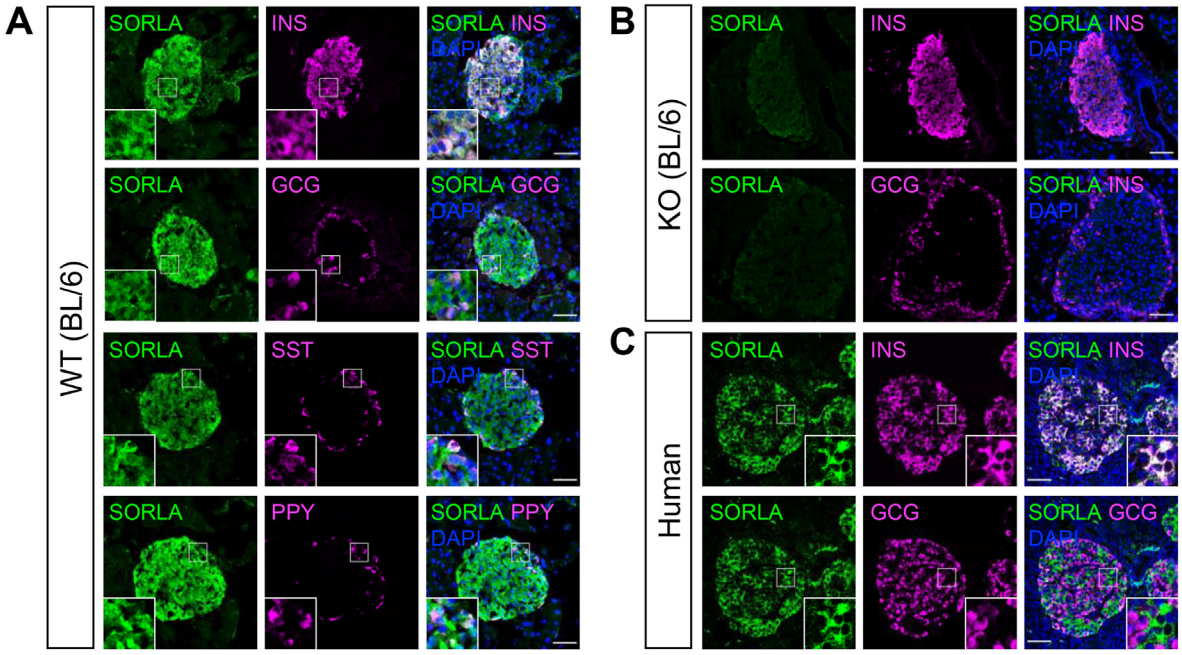

Figure 1: Expression of SORLA in murine and human pancreatic islets. (**A, B**) Immunofluorescence staining of pancreatic sections from (A) WT (BL/6) and (B) SORLA KO (BL/6) mice for SORLA (green), insulin (INS, magenta), glucagon (GCG, magenta), somatostatin (SST, magenta), and pancreatic polypeptide (PPY, magenta). Nuclei were counterstained with DAPI (blue). Prominent expression of SORLA is seen in WT but not SORLA KO islets. (**C**) Immunodetection of SORLA (green) and insulin or glucagon (magenta) on representative sections of human pancreatic biopsies from three non-diabetic patients. Single and merged channel configurations are shown. The insets depict higher magnifications of the areas indicated by white boxes in the overview images. Scale bars, 50 μm.

transgenic line expressing hIAPP under the control of the rat insulin II promoter (on an FVB/N background) [23,24]. Male mice hemizygous for the *hIAPP* transgene and genetically deficient for *Sorl1* (hIAPP:SORLA KO), as well as hIAPP-expressing control animals (hIAPP:SORLA WT) were selected for analysis. We also generated non-transgenic control groups (SORLA WT, SORLA KO) to assess the impact of SORLA deficiency on glucose homeostasis in the absence of the *hIAPP* transgene. In addition to age, dietary stress imposed by high-fat diet (HFD) feeding contributes to islet amyloid formation [25]. Therefore, we performed our studies in mice fed a normal chow diet (ND) or a HFD (60% crude fat) for 6 months, starting at 4 weeks of age. We first examined the effects of SORLA deficiency on islet amyloid deposition by staining pancreatic tissue sections from 7-month old hIAPP:SORLA WT and hIAPP:SORLA KO mice with thioflavin S (ThioS) (Figure 2A). Remarkably, the prevalence of islet amyloid deposition was significantly higher in hIAPP:SORLA KO mice compared to WT mice on ND (WT 17.3 $\pm$ 4.7% vs KO 70.3 $\pm$ 9.7% amyloid containing islets, $p < 0.0001$) (Figure 2B). The protective effect of SORLA against islet amyloid prevalence was maintained under HFD (WT 44.2 $\pm$ 8.0% vs KO 71.8 $\pm$ 7.8% amyloid containing islets, $p = 0.035$) (Figure 2B). Furthermore, the severity of islet amyloid was significantly increased in ND-fed hIAPP:SORLA KO mice as compared to WT mice, which developed almost no islet amyloid (WT 0.56 $\pm$ 0.16% vs KO 6.9 $\pm$ 1.8% ThioS positive area of total islet area, $p = 0.019$) (Figure 2C). However, no significant difference in amyloid severity between hIAPP:SORLA WT and KO mice was seen when animals were fed a HFD (WT 2.9 $\pm$ 0.8% vs KO 7.8 $\pm$ 2.6% ThioS positive area of total islet area, $p = 0.0798$) (Figure 2C). This lack of SORLA protection under HFD may be attributed to an already aggravated amyloid burden in SORLA-deficient mice and blunted response under dietary stress.

Islet amyloid is associated with apoptotic cell death and impaired beta cell function. Accordingly, we performed TUNEL staining to test whether the increased islet amyloid observed in SORLA-deficient mice also correlated with increased cell death (Figure 2D). Compared to hIAPP:SORLA WTs, the percentage of apoptotic cells per islet was significantly higher in the ND-fed hIAPP:SORLA KO mice. Consistent with data on islet amyloid severity, this effect of SORLA-deficiency was not seen in mice fed a HFD (Figure 2E). Amyloid deposition as a possible cause of islet cell death in SORLA mutant mice was substantiated by linear regression analysis, which demonstrated a positive correlation between the severity of islet amyloid and extent of apoptosis (Figure 2F). We attempted to further identify the islet cell type mainly impacted by apoptosis by co-staining for insulin or glucagon. However, as exemplified in the representative images in Figure 2D, TUNEL positive cells mostly lack staining for these hormones, suggesting loss of hormone expression as a consequence of pathology. A lack of insulin expression was also observed in islet areas positive for ThioS amyloid staining (Figure 2A). Because hIAPP:SORLA KO islets showed a trend towards reduced insulin positive islet area (Figure S1B, ND: WT 59.2 $\pm$ 1.2% vs KO 56.3 $\pm$ 1.1%, $p = 0.10$), while glucagon positive islet area was comparable between SORLA genotypes (Figure S1C, ND: WT 11.3 $\pm$ 0.5% vs KO 11.3 $\pm$ 0.9%, $p = 0.97$), we suspect apoptotic cells are likely to be beta cells.

Although SORLA deficiency increased amyloid burden and cell death in ND-fed hIAPP-expressing mice, no significant differences in their overall islet morphology, including total islet area as well as alpha and beta cell areas were observed between genotypes (Figure S1A–C). To determine if compensatory upregulation of cell proliferation may account for the maintenance of islet tissue area in receptor-mutant mice, we examined cell proliferation by staining for proliferation marker Ki67

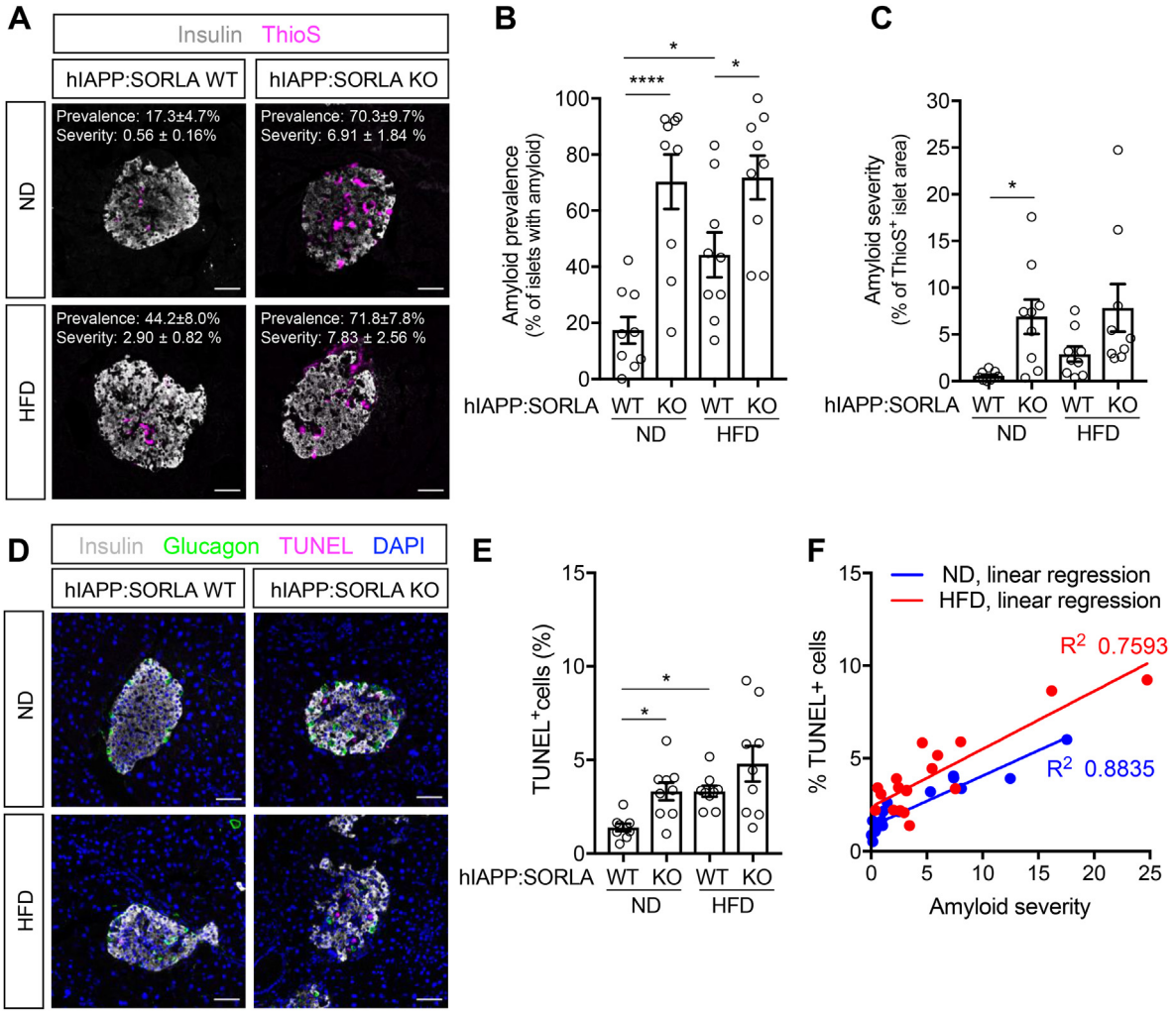

Figure 2: SORLA deficiency promotes islet amyloid deposition and islet cell death in hIAPP-expressing mice. Pancreatic sections from 33- to 35-weeks old mice of the indicated genotypes were examined for (A–C) islet amyloid deposition and (D, E) cell death ($n = 9$ mice per genotype, 20–30 islets per mouse). Animals were fed a normal chow diet (ND) or a high-fat diet (HFD) for 6 months. Scale bars, 50 μm. (**A**) Islet amyloid was assessed by staining with thioflavin S (ThioS, magenta) and immunostaining for insulin (white). Quantifications of (**B**) amyloid prevalence (percentage of islets with amyloid) and (**C**) amyloid severity (percentage of ThioS^{+} amyloid area per islet area) on replicate pancreatic sections as exemplified in panel (A). (**D**) Apoptotic cell death was assessed by TUNEL staining (magenta). Sections were also immunostained for insulin (white) and glucagon (green). Nuclei were counterstained with DAPI (blue). (**E**) Quantification of the percentage of TUNEL^{+} cell per islet on replicate pancreatic sections as exemplified in (D). **(F)** Linear regression analyses documented a positive correlation of islet amyloid severity with apoptotic cell death in islets from hIAPP-expressing mice ($n = 18$). Data are shown as mean ± SEM. Statistical significance of differences was determined by two-way ANOVA with post hoc test. *$p < 0.05$, ****$p < 0.0001$.

(Figure S1D). Overall, few proliferative cells were observed in islets with numbers remaining comparable in ND-fed hIAPP:SORLA WT and KO mice (Figure S1E).

Together, these findings indicate that hIAPP:SORLA KO mice at 7 months of age likely represent an early stage of islet amyloid formation towards a trajectory of severe islet pathology.

3.3. Glucose metabolism and beta cell function of hIAPP-expressing SORLA KO mice

In addition to histological assessments of islet amyloid burden, we also monitored the metabolic consequences of SORLA deficiency in both hIAPP-transgenic and non-transgenic mice over time. Since the rat insulin II promoter used to drive beta cell expression of the *hIAPP* transgene was reported to also induce transgene expression in the hypothalamus [26], we examined whether such undesirable expression of *hIAPP* in the brain was present in our mouse models using qPCR. Gene expression analysis demonstrated robust expression of *hIAPP* in islets of hIAPP-transgenic mice. However, no *hIAPP* transcripts were detectable in the hypothalamus or brain cortex of these animals (Suppl. Table 2). This data ensured that metabolic characterizations in our models were not confounded by off-target expression of *hIAPP* in the brain.

At 30 weeks of age, hIAPP:SORLA KO mice on a ND grew slightly heavier than hIAPP:SORLA WT animals (Figure 3A, WT 37.4 ± 1.2 g vs KO 41.8 ± 1.6 g, p = 0.03). However, SORLA deficiency did not impact fasting blood glucose levels, regardless of *hIAPP* transgene expression (Figure 3B). Expression of hIAPP resulted in impaired glucose tolerance when compared with non-transgenic controls (Figure 3C), while SORLA KO animals showed normal glucose tolerance compared to WT controls (Figure 3C). Additionally, we determined

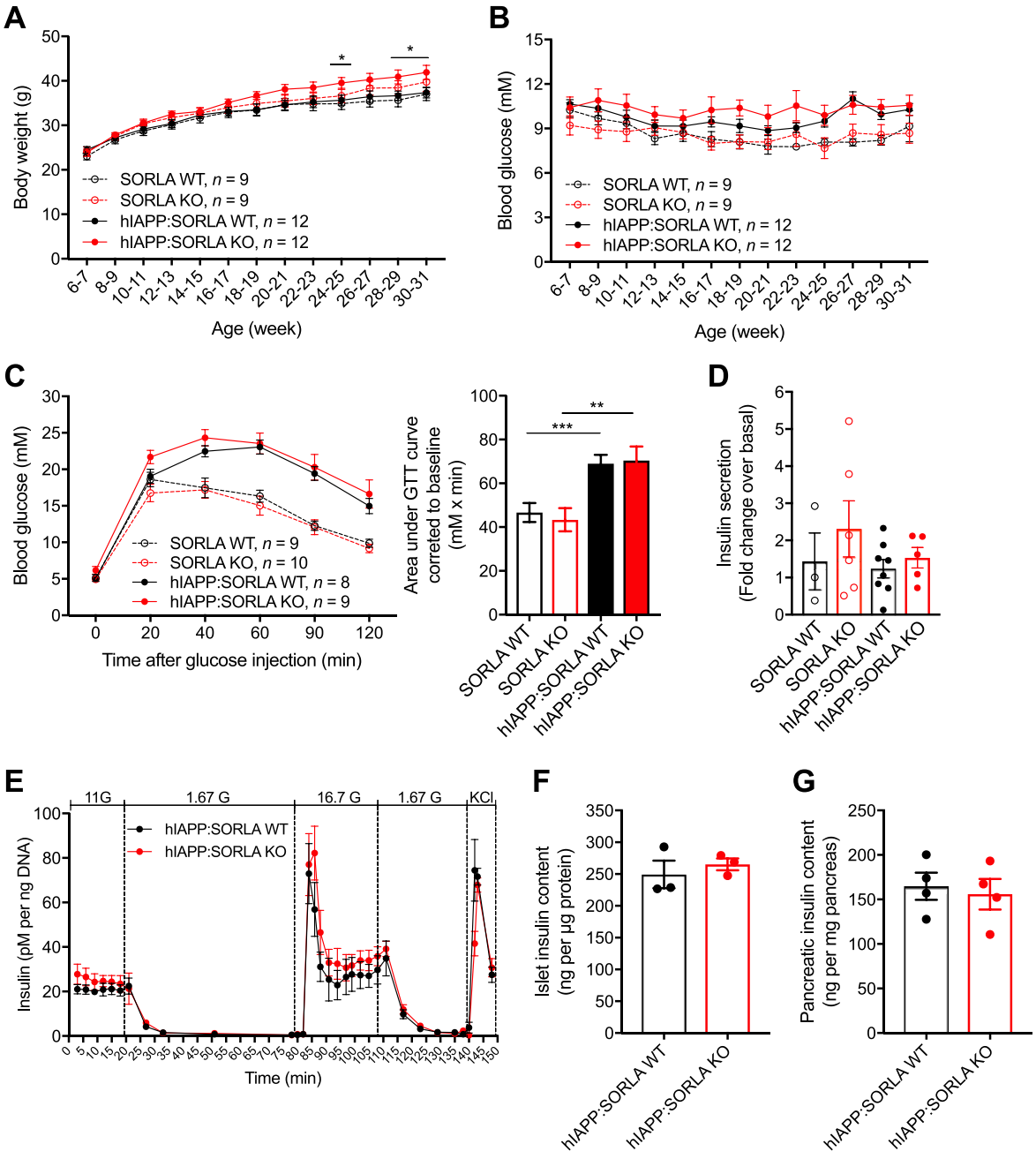

Figure 3: Metabolic characterization and beta cell function of hIAPP-expressing wildtype and SORLA-deficient mice on a normal chow diet. (**A and B**) Bi-weekly (A) body weight and (B) 6 h fasting blood glucose measurements of mice of the indicated genotypes. **(C)** Glucose tolerance test (GTT) performed in 30- to 32-weeks old mice after a 16 h fast via intraperitoneal glucose injection (2 g/kg). Response to glucose clearance was quantified based on area under the curve. **(D)** Glucose-stimulated insulin secretion (GSIS) was assessed in 31- to 33-weeks old mice of the indicated genotypes. A glucose dose of 2 g/kg was administered intraperitoneally after a 16 h fast. Data are represented as fold change in insulin secretion at 30 min post-glucose injection compared to basal levels. **(E)** Dynamic GSIS was tested on perifused islets from 31- to 33-weeks old hIAPP-expressing SORLA WT or KO mice ($n = 3$ mice per genotype, with technical duplicates). (**F and G**) Quantifications of insulin content in (F) isolated islets (n = 3) and (G) whole pancreas (n = 4) of hIAPP-expressing SORLA WT or KO mice. Data are shown as mean ± SEM. Statistical significance of differences (A, C) was determined by unpaired Student's t-test. $^{**}p < 0.01$, $^{***}p < 0.001$.

the effect of SORLA deficiency on beta cell function by measuring glucose-stimulated insulin secretion (GSIS) in mice (Figure 3D) and isolated islets (Figure 3E). The fold change in insulin secretion upon intraperitoneal glucose administration was similar between SORLA genotypes (Figure 3D). Similarly, SORLA deficiency did not significantly impact glucose- or KCl-stimulated insulin secretion in perifusion experiments of islets from hIAPP-expressing mice (Figure 3E). Furthermore, there were no significant differences in insulin content in both isolated islets (Figure 3F) nor pancreas (Figure 3G) between SORLA genotypes.

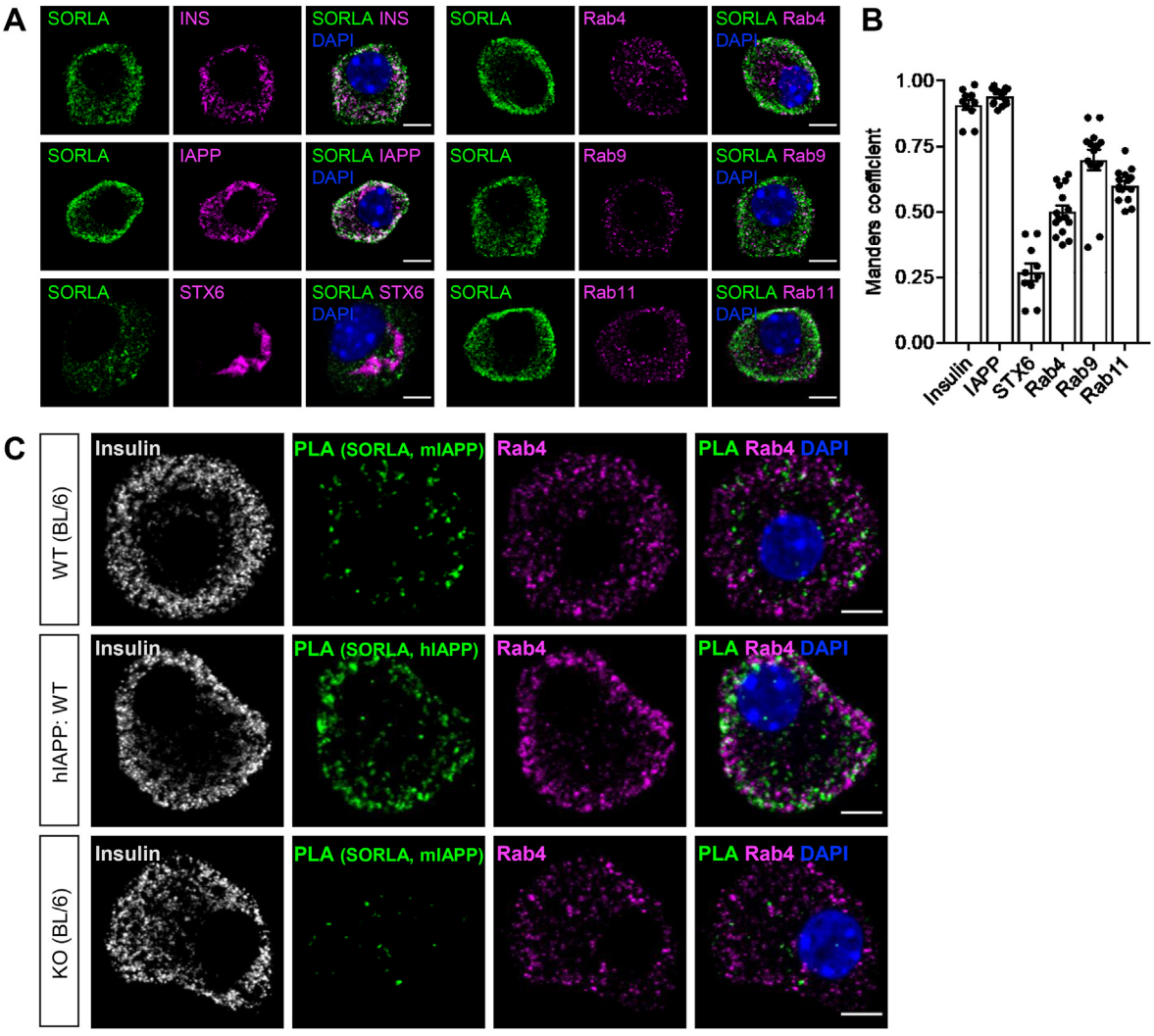

Figure 4: SORLA co-localizes with IAPP to the endocytic compartment of islet beta cells. (A) Dispersed islet cells from WT(BL/6) mice were immunostained for SORLA (green) and the following cell compartment markers (magenta): insulin, INS or IAPP (secretory vesicles), syntaxin-6 (STX6; *trans*-Golgi), Rab4 (early endosomes), Rab9 (late endosomes), or Rab11 (recycling endosomes). Nuclei were counterstained with DAPI. Single and merged channel configurations are shown. Scale bars, 5 μm. **(B)** Degree of co-localization between SORLA and each compartment marker was quantified by Manders' co-localization coefficient ($n = 10–15$ cells). **(C)** Proximity ligation assay detected close proximity of SORLA and mouse or human IAPP (green) in dispersed islet cells from WT(BL/6) or hIAPP:SORLA WT mice. Cells were additionally immunostained for insulin (white), Rab4 (magenta), and nuclei counterstained with DAPI (blue). Single as well as merged channel configurations are shown. Scale bars, 5 μm. Data are shown as mean ± SEM.

To further determine if SORLA promotes the development of diabetes (dependent or independent of hIAPP), we challenged mice with HFD for an extended period of 6 months starting at 4 weeks of age. SORLA-deficient mice also grew heavier on HFD compared to their WT littermates (Figure S2A). Yet, similar to ND-fed mice, SORLA-deficient animals and their WT littermates on HFD had comparable fasting blood glucose levels (Figure S2B). At 30–32 weeks of age, hIAPP:SORLA KO mice trended to show signs of impaired glucose tolerance, but this finding did not reach statistical significance (Figure S2C). We suspect this slightly impaired glucose tolerance to be attributed to their increased body weight, as there were no observable differences in i*n vivo* glucose-stimulated insulin secretion when compared to hIAPP:SORLA WT mice (Figure S2D).

Taken together, our *in vivo* data demonstrated that loss of SORLA promotes islet amyloid burden and islet cell loss without overt impact on blood glucose homeostasis. This defect was observed in normal chow-fed mice and did not require any additional dietary stressor. These findings suggest a possible role for SORLA in regulating amyloid development under physiological conditions and early stages of diabetes pathology.

3.4. Loss of SORLA does not alter proIAPP processing

Next, we explored the molecular mechanism whereby SORLA controls IAPP handling and islet amyloid deposition. Since impaired processing of proIAPP has been implicated in islet amyloid formation [1,7,27], we initially tested whether SORLA may function as an intracellular sorting receptor regulating IAPP maturation in islet beta cells, similar to its function in sorting APP in neurons [10,15]. Accordingly, we measured fasting plasma levels of proh$IAPP_{1\text{-}48}$ and mature hIAPP in our mouse models by ELISA and calculated the ratio of pro- to mature hIAPP as an

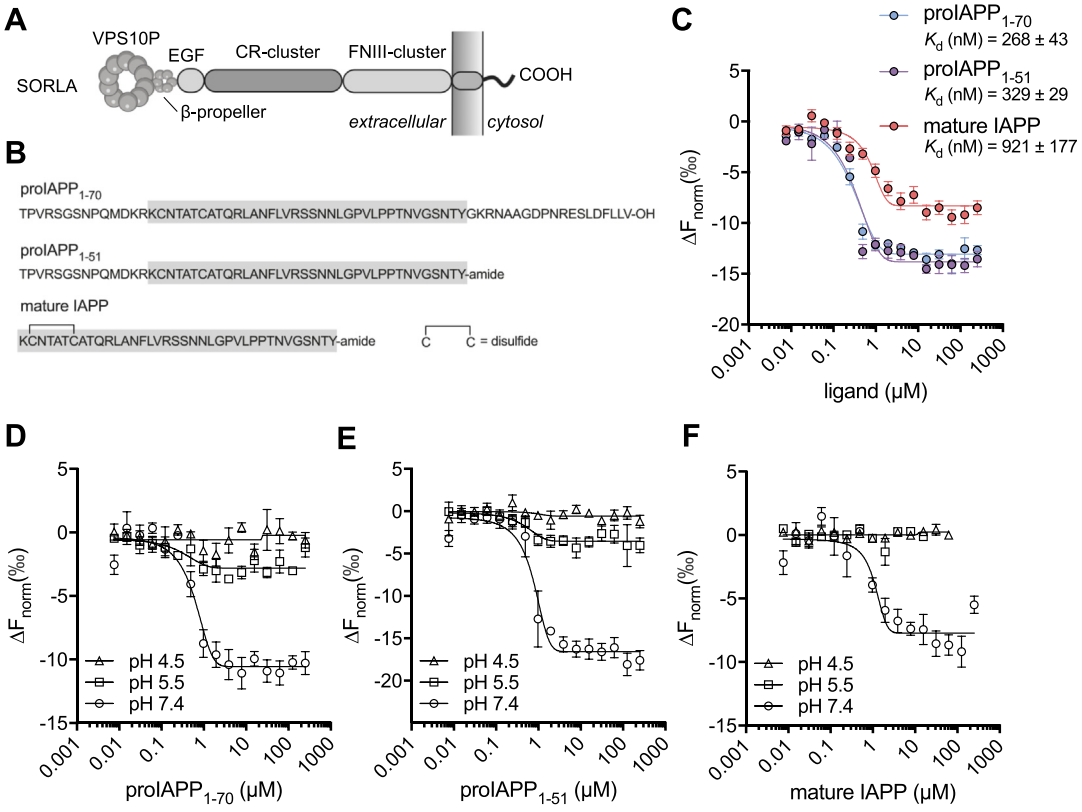

Figure 5: SORLA preferentially binds proIAPP in a pH-dependent manner. (A) Structural domains of SORLA, including vacuolar protein sorting 10 protein (VPS10P) domain, β-propeller, epidermal growth factor (EGF) repeats, fibronectin type III (FNIII) domain, and clusters of complement-type repeats (CR). **(B)** Amino acid sequences of murine proIAPP$_{1-70}$, proIAPP$_{1-51}$, and mature IAPP peptides. **(C)** Binding characteristics between the ectodomain of SORLA and murine IAPP peptides. The His-tagged ectodomain of human SORLA was recombinantly produced in HEK293-EBNA cells and purified using Ni^{2+} affinity chromatography [10]. Binding of different forms of IAPP peptide to the ectodomain of SORLA was determined by microscale thermophoresis (MST) at pH 7.4. The concentration of the fluorescently-labeled SORLA ectodomain was kept constant (3 nM), while non-labeled IAPP was serially titrated from 7.6 nM–250 μM. The change in thermophoresis is expressed as fluorescence intensity normalized to the lowest concentration of labeled IAPP ligand (y-axis = ΔF_{norm}(%0)). Average K_d was derived from at least three independent experiments. Data are shown as mean ± SEM. **(D–F)** Binding of (D) proIAPP$_{1-70}$, (E) proIAPP$_{1-51}$, and (F) mature IAPP to the SORLA ectodomain was tested by MST at pH 4.5, 5.5, and 7.4 as detailed in (C).

indicator of processing efficiency. Both hIAPP-expressing SORLA WT and KO mice had similar levels of mature hIAPP, prohIAPP$_{1-48}$, and ratio of pro- to mature hIAPP, regardless of ND (Figure S3A–C) or HFD (Figure S3D–F) feeding. To further validate these *in vivo* results, we measured levels of secreted mature hIAPP and prohIAPP$_{1-48}$ from isolated islets in standard glucose culture (11 mM), and following low (1.67 mM) or high glucose (16.7 mM) conditions (Figure S3G). No significant differences in the amounts or ratios of secreted mature hIAPP and prohIAPP$_{1-48}$, (Figure S3H–J), nor in total islet content of mature and prohIAPP$_{1-48}$ (Figure S3K, L), were noted in SORLA genotypes across all conditions. These data suggest that SORLA does not impact proIAPP processing, neither directly nor indirectly.

3.5. SORLA is a receptor for soluble IAPP

Prior studies in various cell types have shown that SORLA mainly localizes to the Golgi, cell surface, and endosomes, in line with its function in sorting cargo between plasma membrane, secretory and endocytic compartments [28]. We tested if SORLA localizes to similar subcellular compartments in beta cells by immunostaining for SORLA and organelle markers in dispersed islet cells from WT (BL/6) mice (Figure 4A). Quantification of double-immunostained cells using Manders' co-localization coefficient showed that SORLA most highly co-localized with secretory granule markers (insulin and IAPP); moderately with early (Rab4), late (Rab9), and recycling endosomes (Rab11); and to a lesser extent with the *trans*-Golgi network (STX6) (Figure 4B). We performed proximity ligation assays (PLA) to substantiate close spatial proximity of SORLA with murine IAPP in any of these cell compartments in primary islet beta cells. In these studies, PLA signals were observed distinctly around the cell periphery and in the vicinity of the early endosome marker Rab4 (Figure 4C, top panels). To ascertain that SORLA interacts similarly with murine and human IAPP, we repeated the same experiment on dispersed islet cells from hIAPP-expressing WT animals (Figure 4C, middle panels), showing comparable PLA patterns for both mouse and human IAPP. As expected, no interactions between SORLA and IAPP were detected in cells deficient in SORLA (Figure 4C, bottom panels). Together, these results suggest a prominent interaction of SORLA with IAPP in early endosomes, potentially by acting as an endocytic receptor for the peptide.

To examine whether SORLA was able to act as a receptor for pro- or mature forms of IAPP, we tested their binding interactions using microscale thermophoresis (MST). In this experiment, we used a His-tagged version of the human SORLA ectodomain (Figure 5A), recombinantly expressed and purified from HEK293-EBNA cells [10]. Ligand binding of the ectodomain was tested using commercially synthesized forms of mouse IAPP, namely N-terminally extended proIAPP

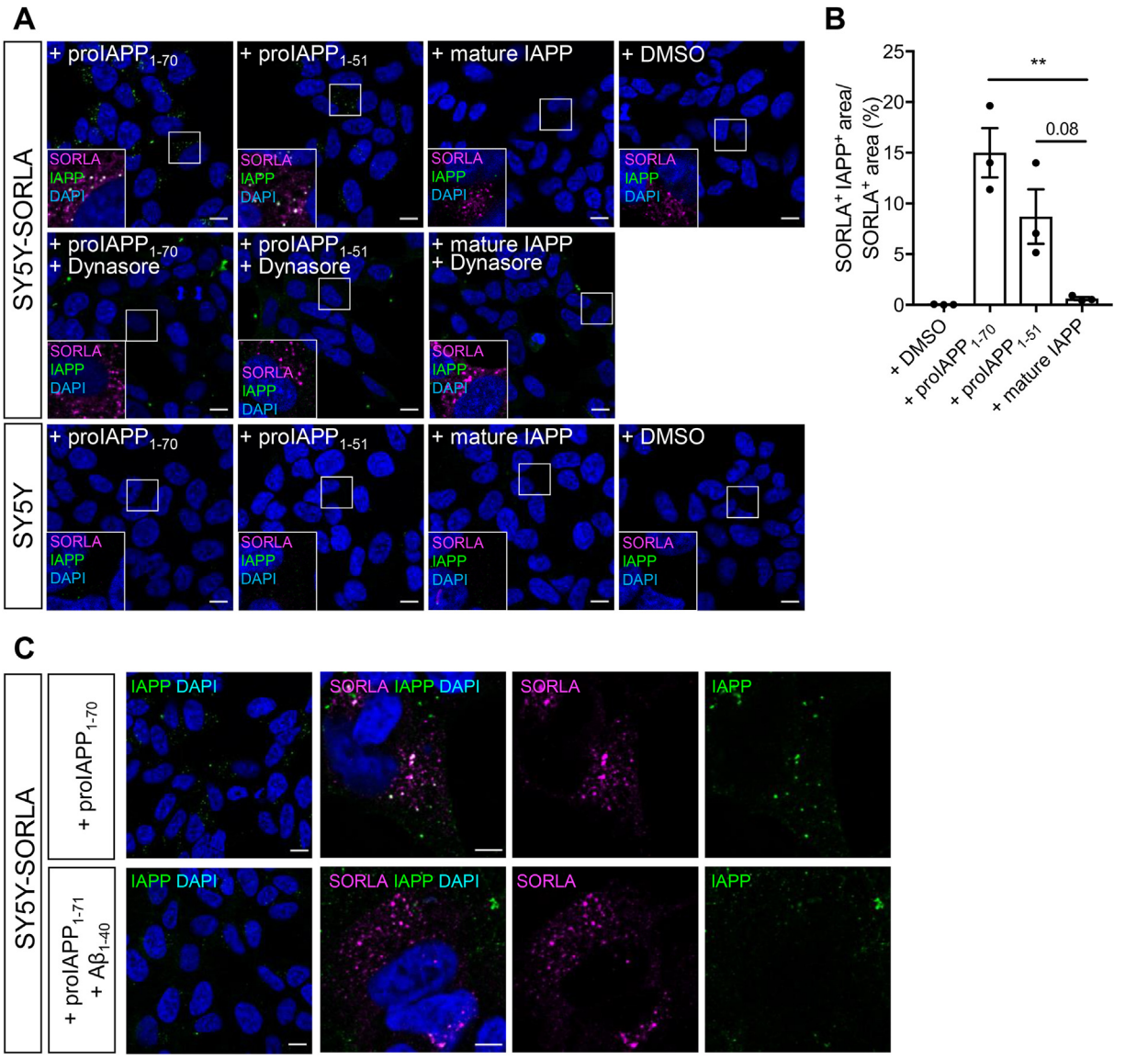

Figure 6: SORLA mediates endocytic uptake of proIAPP, but not mature IAPP. (A) SY5Y cells stably overexpressing SORLA (top, middle panels) and parental SY5Y cells (bottom panel) were incubated with 20 μM of proIAPP$_{1-70}$, proIAPP$_{1-51}$, or mature IAPP peptides, or with 0.1% DMSO (solvent control). Where indicated, cells were also treated with 100 μM dynasore to block dynamin-mediated endocytosis. After 30 min, the cells were fixed and immunostained for SORLA (magenta) and IAPP (green). Nuclei were counterstained with DAPI. The insets depict higher magnifications of the areas indicated by white boxes in the overview images. Scale bars, 10 μm. **(B)** The amount of internalized IAPP peptides was quantified based on the percentage of SORLA immunosignals co-localizing with IAPP peptides ($n = 3$ independent experiments, each with 3–4 images per condition). **(C)** Competition of proIAPP$_{1-70}$ uptake in SY5Y-SORLA cells by Aβ$_{1-40}$. Cells were treated with 20 μM proIAPP$_{1-70}$ alone or in the presence of 100 μM Aβ$_{1-40}$ for 30 min. Presence of SORLA and internalized proIAPP$_{1-70}$ in cells were then immunolabeled by anti-SORLA (magenta) and anti-IAPP antibodies (green), respectively, and nuclei counterstained with DAPI (blue). Representative images from three independent experiments. Scale bars, 5 μm. Data are shown as mean ± SEM. Statistical significance of differences in (B) was determined by one-way ANOVA with post hoc test. **$p < 0.01$.

(proIAPP$_{1-70}$), C-terminally extended proIAPP (proIAPP$_{1-51}$), or mature IAPP peptides (Figure 5B). Mouse IAPP peptides were used in these experiments as they exhibit better solubility and stability *in vitro* as compared to the aggregation-prone human peptides [29]. This strategy enabled us to determine if SORLA interacts with nascent soluble IAPP, preceding misfolding and fibrillation. Binding interactions were detected by comparing multiple measurements over a temperature gradient, with a constant concentration of fluorescently-labeled SORLA ectodomain and a serial titration of unlabeled IAPP peptides. By performing affinity analysis using K_d model of fit, the SORLA ectodomain was shown to interact with all three forms of IAPP (Figure 5C). However, binding was substantially stronger to the unprocessed forms (proIAPP$_{1-70}$ $K_d \sim 268 \pm 43$ nM; and proIAPP$_{1-51}$ $K_d \sim 329 \pm 29$ nM) as compared to a relatively weaker interaction with mature IAPP ($K_d \sim 921 \pm 177$ nM). The ability to discharge bound cargo in the acidic milieu of endosomes is a characteristic feature of endocytic

receptors, including SORLA [14]. In line with this observation, binding of IAPP peptides to SORLA was strongest at pH 7.4, weaker at pH 5.5, and absent at pH 4.5 (Figure 5D–F).

3.6. SORLA mediates endocytosis of proIAPP, but not mature IAPP

The above data indicated that SORLA may act as a receptor for monomeric IAPP peptides, possibly delivering them to lysosomal catabolism. To corroborate this hypothesis, we tested the ability of SORLA to mediate endocytic uptake of IAPP *in vitro*. Here, we assessed mouse IAPP peptide uptake in a neuroblastoma SH-SY5Y cell line stably overexpressing SORLA. This cell line is commonly used to study SORLA-mediated sorting functions [10,15]. Moreover, this cell line does not express endogenous IAPP (Figure 6A, DMSO panel), enabling us to examine cellular uptake of unlabeled, synthetic IAPP peptides.

Evaluating cellular uptake of exogenously added IAPP peptides in SY5Y cells expressing SORLA, intracellular accumulation was seen for $proIAPP_{1\text{-}70}$ and $proIAPP_{1\text{-}51}$, but not for mature IAPP (Figure 6A, top panels). Quantifications showed that $proIAPP_{1\text{-}70}$ was the most readily internalized species in the presence of SORLA (Figure 6B). SORLA-dependent uptake of the proIAPP peptides was inhibited by treatment with dynasore, an inhibitor of clathrin-mediated endocytosis (Figure 6A, middle panels). No uptake was seen in parental SY5Y cells lacking SORLA expression (Figure 6A, bottom panels).

Since SORLA is known to bind small peptides, including Aβ, via its VPS10P domain [30], we next tested if $proIAPP_{1\text{-}70}$ also binds to the same region in the receptor's ectodomain. We found that the level of internalized $proIAPP_{1\text{-}70}$ in SORLA-expressing SY5Y cells was significantly reduced in the presence of a 5-fold molar excess of Aβ (Figure 6C), indicating that $proIAPP_{1\text{-}70}$ and Aβ compete for the same binding site in SORLA.

Finally, immunostaining revealed that internalized proIAPP peptides were predominately directed to early endosomes (EEA1, 89.9%) (Figure 7A,B). To identify whether endocytosed peptides were further transported to lysosomes for degradation, or to the TGN for recycling, we co-stained with a lysosomal dye (LysoTracker) or TGN38, respectively. Our results showed that proIAPP peptides co-localize more with lysotracker (51.6%) than with TGN38 (25.2%) (Figure 7A,B), arguing for delivery to lysosomes rather than the TGN recycling of internalized propeptides.

4. DISCUSSION

Overproduction or hypersecretion of IAPP under conditions of increased insulin demand have been proposed as underlying mechanisms of islet amyloid formation. However, excessive formation of the peptide alone is insufficient to promote islet amyloid formation, as evidenced by the lack of islet amyloid found in hIAPP transgenic mice or non-diabetic individuals with hyperinsulinemia [31,32]. Thus, alternative mechanisms are likely involved in maintaining IAPP homeostasis and minimizing its propensity to form amyloid. We have identified a unique cellular pathway that counteracts the initial stages of IAPP aggregation. In our model, SORLA acts as a clearance receptor specific for soluble,

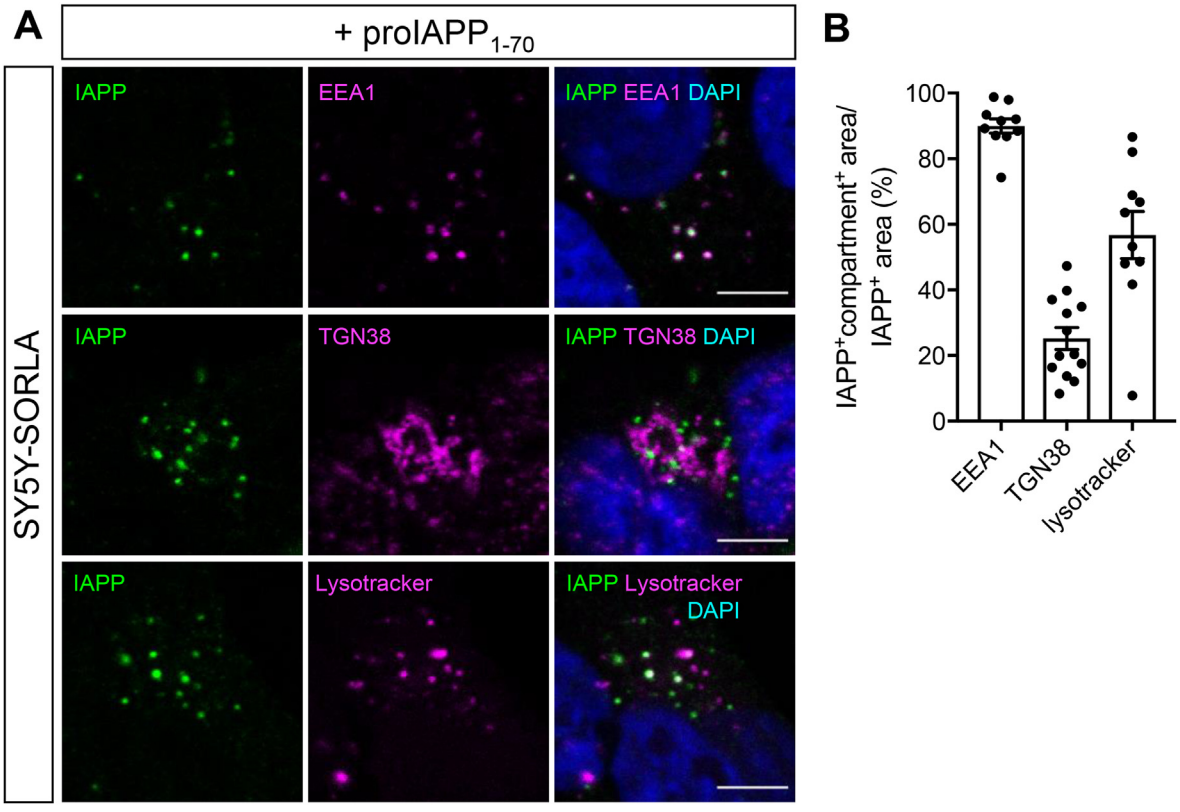

Figure 7: SORLA delivers proIAPP towards endolysosomal compartments. (A) SY5Y-SORLA cells were treated with 20 μM $proIAPP_{1\text{-}70}$ for 30 min as described in Figure 6A. Subsequently, the cells were immunostained for IAPP (green) and compartment makers EEA1 and TGN38 (magenta). Lysosomes were labeled by preincubating cells with Lysotracker Deep Red (magenta) for 1 h prior to uptake assay. Nuclei were counterstained with DAPI (blue). Scale bars, 5 μm. (**B**) Quantifications of object-based colocalization between internalized $proIAPP_{1\text{-}70}$ and each compartment marker ($n = 10–13$ images per marker).

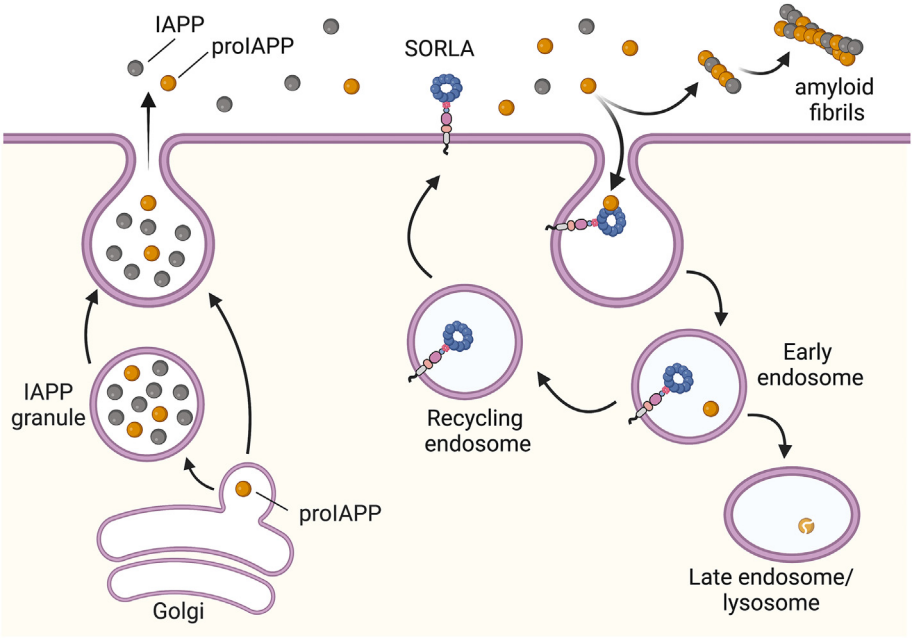

Figure 8: Model for SORLA-mediated endocytosis of proIAPP. SORLA functions as an endocytic receptor for clearance of pro- but not mature IAPP released from islet beta cells. Following pH-dependent release of proIAPP in early endosomes, SORLA recycles back to the cell surface, whereas proIAPP is destined for lysosomal degradation. SORLA-mediated clearance of proIAPP released from cells counteracts pancreatic amyloid fibril formation. Created with BioRender.

monomeric proIAPP released from islet beta cells. Receptor-mediated endocytosis of proIAPP delivers it to lysosomal catabolism, reducing its extracellular buildup and aggregation into fibrils, thereby protecting islets from amyloid-induced cell death (Figure 8).

The cellular pathways for IAPP biosynthesis are complex, involving movement of nascent proIAPP along the biosynthetic route from the endoplasmic reticulum to the Golgi, as well as transport of its partially processed proIAPP intermediate to secretory granules for final processing and maturation. Extensive studies have identified prohormone convertases (PC1/3 and PC2) [33,34], peptidyl-glycine alpha-amidating monooxygenase (PAM) [35] and carboxypeptidase E (CPE) [36] as key regulators of proIAPP processing and post-translational modification. However, the identity of a sorting receptor responsible for transporting IAPP along its biosynthetic pathway remains unknown. CPE has been proposed to carry additional function as a sorting receptor for directing prohormones, including proinsulin, to the regulated secretory granules [37]. However, conflicting results from other studies have challenged the role of CPE as a prohormone sorting receptor [38]. Following a hypothesis-driven approach, we therefore explored a possible role for the VPS10P domain receptor SORLA in IAPP transport. VPS10P domain receptors are a distinct class of sorting receptors that direct intracellular trafficking and processing of proteins along the secretory and endocytic paths of cells [39]. With relevance to islet biology, the VPS10P domain receptor SorCS1 directs replenishment of secretory granules with insulin [40], providing a molecular explanation for its association with type 2 diabetes in humans and mice [41,42]. While our data dispute a similar function for SORLA in intracellular sorting and release of IAPP (Figure S3), they reveal a surprising role for this receptor in the clearance of extracellular soluble proIAPP (Figure 6). SORLA-mediated proIAPP clearance is blocked by dynasore, indicating a clathrin-dependent mechanism of uptake. In addition, internalized proIAPP molecules are preferentially sorted to endolysosomal compartments (Figure 7), suggesting that they are destined for lysosomal catabolism. In support of this assumption, binding of IAPP to SORLA is lost at low pH (Figure 5). pH dependency of binding is a hallmark of endocytosis, enabling receptors to discharge their cargo in acidified endosomes. Because of a low endocytic activity of islet beta cells *in vitro*, we have not been able to directly document SORLA-dependent uptake of proIAPP in this cell type. However, predominant localization of SORLA to early, late, and recycling endosomes in isolated beta cells (Figure 4) suggests a similar endocytic receptor function as in SY5Y cells.

Our observation that SORLA-mediated uptake of soluble, monomeric proIAPP is impaired by Aβ (Figure 6C) indicates that proIAPP binds to the same site as Aβ in a funnel formed by the VSP10P domain, a 700 amino acid module shared by the ectodomains of all VSP10P domain receptors [43]. Importantly, the affinity of SORLA is higher for the pro- compared to the mature form of the peptide ($K_d \sim 300$ vs. 921 nM), explaining its ability to clear pro- but not mature IAPP. This observation is noteworthy, as it addresses an open question concerning the origin of islet amyloid. Loss of the proIAPP receptor SORLA increases islet amyloid deposition in mice (Figure 2). This finding supports earlier hypotheses that proIAPP is likely a critical species in initiating early steps of amyloid deposition [7,44]. There have also been debates on the extracellular or intracellular origin of islet amyloid [45–47]. Our model of SORLA-mediated endocytosis of proIAPP provides new evidence to support islet amyloid formation in the extracellular space as a consequence of aberrant accumulation of secreted IAPP.

As a caveat, we have not directly tested binding of human IAPP peptides to SORLA, as their enhanced propensity for aggregation *in vitro* precluded analysis by microscale thermophoresis. Human IAPP differs from murine IAPP in its amyloidogenicity due to differences in the amino acid sequence at position 20–29 of the mature IAPP peptide [48]. In addition, there are differences in the amino acid sequence of flanking propeptide regions between human and mouse IAPP amino

acid sequences, which may also impact amyloidogenicity and/or protein—protein interactions. Therefore, documenting direct binding between SORLA and human IAPP remains an open question. Still, our findings document comparable close proximity of SORLA with mouse and human IAPP in islet beta cells and shared colocalization patterns in the vicinity of early endosomal compartment (Figure 4C). Furthermore, the obvious impact of SORLA deficiency on islet amyloid formation in transgenic mice expressing human IAPP (Figure 2A) provides encouraging evidence to support a role of SORLA in control of human IAPP metabolism.

Significant amounts of islet amyloid are already present in normal chow-fed hIAPP-expressing mice lacking SORLA, but not in wildtype control. This finding is surprising as previous studies on hIAPP transgenic mice reported no spontaneous islet amyloidosis unless additional diabetogenic traits, such as obesity or insulin resistance, were introduced genetically [49], pharmacologically [23] or through dietary interventions [50]. Our data suggest that SORLA has an important role in maintaining IAPP homeostasis under physiological conditions. This protective effect against islet amyloid is blunted under conditions of dietary stress, possibly because it is masked by hypersecretion of hIAPP following HFD feeding, especially in our transgenic mouse model which overexpresses supraphysiological levels of human IAPP (Figure S3D,E). This saturating effect of overexpression may also explain the lack of changes in circulating plasma proIAPP levels in SORLA-deficient hIAPP transgenic mice. Still, the lack of an overt impact of SORLA deficiency on systemic glucose homeostasis (Figure 3) suggests that the effects on proIAPP uptake and islet amyloid formation are likely attributed to a loss of islet-specific receptor activities.

The severity of islet amyloid deposition correlates with beta cell dysfunction, apoptosis, and hyperglycemia [21,51,52]. *In vitro* studies have demonstrated that synthetic hIAPP-induced amyloid fibrils are toxic to beta cells in cultured islets [53], and that pharmacological inhibition of hIAPP fibril formation improves viability of cultured islets [54]. In the present study of 7-month-old animals, we observed aggravated cell death in islets of hIAPP-expressing SORLA-deficient mice *in vivo*, in line with enhanced islet amyloid in these animals. However, cell death did not progress to overt beta cell dysfunction and impairment in glucose metabolism under the experimental conditions tested here. At present, we cannot conclude whether changes in experimental procedures, such as extending the observational period by an additional 6 months or further increasing the number of biological replicates may uncover an overt islet dysfunction in mutant mice. Still, the observed increase in cell death can be expected to have negative impacts on islet function in SORLA deficient mice at an older age when mice develop prolonged chronic metabolic stress, following further accumulation of amyloid deposits.

In conclusion, our studies have identified a protective role for SORLA against amyloid development not only in the brain, but also in islet beta cells through mediating catabolism of the aggregation-prone peptide ligands. Future studies will corroborate whether this receptor plays a similarly important role in glucose homeostasis and onset of diabetes as it does in neurodegeneration and risk of AD.

FUNDING

Studies were funded in part by a Helmholtz Graduate School fellowship at Max-Delbrück-Center (MDC) to AZLS, and a JDRF postdoctoral fellowship (#3-PDF-2017-373-A-N) to YCC. Further funding was provided by the Canadian Institutes of Health Research Operating grant (PJT-153156) to CBV, and the European Research Council (BeyOND No. 335692), the Alzheimer Forschung Initiative (#18003), and the Novo Nordisk Foundation (NNF18OC0033928) to TEW.

CONTRIBUTION STATEMENT

AZLS conceived and designed the study, performed experiments, collected, analyzed and interpreted data. YCC performed experiments, collected and analyzed data on human IAPP ELISAs. TS and AS contributed to the use of, experimental design, and data interpretation of automated islet perifusion assays. ES provided tissue sections on human pancreatic biopsies. CBV contributed to the design of experiments, interpreted data and provided critical reagents for human IAPP ELISA. TEW contributed to the design of experiments, interpreted data and provided critical reagents. AZLS and TEW wrote the manuscript with editorial input, review and approval for publication from all authors. AZLS and TEW are guarantors of this work.

DATA AVAILABILITY

Data will be made available on request.

ACKNOWLEDGEMENT

We are indebted to C. Kruse and K. Kampf for expert technical assistance and to V. Schmidt-Krüger for help in obtaining animal experimentation licenses. We thank the Advanced Light Microscopy Platform and the Preclinical Research Center of the MDC for technical support and assistance in this work.

CONFLICT OF INTEREST

The authors declare no competing interest related to this manuscript.

APPENDIX A. SUPPLEMENTARY DATA

Supplementary data to this article can be found online at https://doi.org/10.1016/j.molmet.2022.101585.

REFERENCES

[1] Chen, Y.-C., Taylor, A.J., Verchere, C.B., 2018. Islet prohormone processing in health and disease. Diabetes, Obesity and Metabolism 20:64—76. https://doi.org/10.1111/dom.13401.

[2] Marzban, L., Trigo-Gonzalez, G., Verchere, C.B., 2005. Processing of pro-islet amyloid polypeptide in the constitutive and regulated secretory pathways of β cells. Molecular Endocrinology. https://doi.org/10.1210/me.2004-0407.

[3] Lutz, T.A., 2010. The role of amylin in the control of energy homeostasis. American Journal of Physiology - Regulatory, Integrative and Comparative Physiology 298(6). https://doi.org/10.1152/ajpregu.00703.2009.

[4] Gebre-Medhin, S., Olofsson, C., Mulder, H., 2000. Islet amyloid polypeptide in the islets of Langerhans: friend or foe? Diabetologia 43(6):687—695 https://doi.org/10.1007/s001250051364.

[5] Hull, R.L., Westermark, G.T., Westermark, P., Kahn, S.E., 2004. Islet amyloid: a critical entity in the pathogenesis of type 2 diabetes. Journal of Clinical Endocrinology and Metabolism. https://doi.org/10.1210/jc.2004-0405.

[6] Clark, A., Wells, C.A., Buley, I.D., Cruickshank, J.K., Vanhegan, R.I., Matthews, D.R., et al., 1988. Islet amyloid, increased A-cells, reduced B-cells and exocrine fibrosis: quantitative changes in the pancreas in type 2 diabetes. Diabetes Research 9(4):151—159.

[7] Paulsson, J.F., Andersson, A., Westermark, P., Westermark, G.T., 2006. Intracellular amyloid-like deposits contain unprocessed pro-islet amyloid

polypeptide (proIAPP) in beta cells of transgenic mice overexpressing the gene for human IAPP and transplanted human islets. Diabetologia. https://doi.org/10.1007/s00125-006-0206-7.

[8] Courtade, J.A., Wang, E.Y., Yen, P., Dai, D.L., Soukhatcheva, G., Orban, P.C., et al., 2017. Loss of prohormone convertase 2 promotes beta cell dysfunction in a rodent transplant model expressing human pro-islet amyloid polypeptide. Diabetologia. https://doi.org/10.1007/s00125-016-4174-2.

[9] Haass, C., Selkoe, D.J., 2007. Soluble protein oligomers in neurodegeneration: lessons from the Alzheimer's amyloid β-peptide. Nature Reviews Molecular Cell Biology 8(2):101–112. https://doi.org/10.1038/nrm2101.

[10] Andersen, O.M., Reiche, J., Schmidt, V., Gotthardt, M., Spoelgen, R., Behlke, J., et al., 2005. Neuronal sorting protein-related receptor sorLA/LR11 regulates processing of the amyloid precursor protein. Proceedings of the National Academy of Sciences 102(38):13461–13466. https://doi.org/10.1073/pnas.0503689102.

[11] Rogaeva, E., Meng, Y., Lee, J.H., Gu, Y., Kawarai, T., Zou, F., et al., 2007. The neuronal sortilin-related receptor SORL1 is genetically associated with Alzheimer disease. Nature Genetics 39(2):168–177. https://doi.org/10.1038/ng1943.

[12] Lambert, J.C., Ibrahim-Verbaas, C.A., Harold, D., Naj, A.C., Sims, R., Bellenguez, C., et al., 2013. Meta-analysis of 74,046 individuals identifies 11 new susceptibility loci for Alzheimer's disease. Nature Genetics 45(12):1452–1458. https://doi.org/10.1038/ng.2802.

[13] Offe, K., Dodson, S., Shoemaker, J., Fritz, J., Gearing, M., Levey, A., Lah, J., 2006. The lipoprotein receptor LR11 regulates amyloid beta production and amyloid precursor protein traffic in endosomal compartments. Journal of Neuroscience 26(5):1596–1603. https://doi.org/10.1523/JNEUROSCI.4946-05.2006.

[14] Caglayan, S., Takagi-Niidome, S., Liao, F., Carlo, A.S., Schmidt, V., Burgert, T., et al., 2014. Lysosomal sorting of amyloid-β by the SORLA receptor is impaired by a familial Alzheimer's disease mutation. Science Translational Medicine 6(223). https://doi.org/10.1126/scitranslmed.3007747.

[15] Dumanis, S.B., Burgert, T., Caglayan, S., Füchtbauer, A., Füchtbauer, E.M., Schmidt, V., et al., 2015. Distinct functions for anterograde and retrograde sorting of SORLA in amyloidogenic processes in the brain. Journal of Neuroscience 35(37):12703–12713. https://doi.org/10.1523/JNEUROSCI.0427-15.2015.

[16] Pottier, C., Hannequin, D., Coutant, S., Rovelet-Lecrux, A., Wallon, D., Rousseau, S., et al., 2012. High frequency of potentially pathogenic SORL1 mutations in autosomal dominant early-onset Alzheimer disease. Molecular Psychiatry 17(9):875–879. https://doi.org/10.1038/mp.2012.15.

[17] Segerstolpe, Å., Palasantza, A., Eliasson, P., Andersson, E.M., Andréasson, A.C., Sun, X., et al., 2016. Single-cell transcriptome profiling of human pancreatic islets in health and type 2 diabetes. Cell Metabolism 24(4):593–607. https://doi.org/10.1016/j.cmet.2016.08.020.

[18] Neelankal John, A., Ram, R., Jiang, F.X., 2018. RNA-seq analysis of islets to characterise the dedifferentiation in type 2 diabetes model mice db/db. Endocrine Pathology 29(3):207–221. https://doi.org/10.1007/s12022-018-9523-x.

[19] Muraro, M.J., Dharmadhikari, G., Grün, D., Groen, N., Dielen, T., Jansen, E., et al., 2016. A single-cell transcriptome atlas of the human pancreas. Cell Systems 3(4):385–394. https://doi.org/10.1016/j.cels.2016.09.002 e3.

[20] Monti, G., Andersen, O.M., 2018. 20 Years anniversary for SORLA/SORL1 (1996-2016). Receptors & Clinical Investigation 4:1–10. https://doi.org/10.14800/rci.1611.

[21] Verchere, C.B., D'Alessio, D.A., Palmiter, R.D., Weir, G.C., Bonner-Weir, S., Baskin, D.G., et al., 1996. Islet amyloid formation associated with hyperglycemia in transgenic mice with pancreatic beta cell expression of human islet amyloid polypeptide. Proceedings of the National Academy of Sciences of the United States of America 93(8):3492–3496. https://doi.org/10.1073/pnas.93.8.3492.

[22] Courtade, J.A., Klimek-Abercrombie, A.M., Chen, Y.C., Patel, N., Lu, P.Y.T., Speake, C., et al., 2017. Measurementof pro-islet amyloid polypeptide (1-48) in diabetes and islet transplants. Journal of Clinical Endocrinology and Metabolism. https://doi.org/10.1210/jc.2016-2773.

[23] Couce, M., Kane, L.A., O'Brien, T.D., Charlesworth, J., Soeller, W., McNeish, J., et al., 1996. Treatment with growth hormone and dexamethasone in mice transgenic for human islet amyloid polypeptide causes islet amyloidosis and β-cell dysfunction. Diabetes. https://doi.org/10.2337/diab.45.8.1094.

[24] Janson, J., Soeller, W.C., Roche, P.C., Nelson, R.T., Torchia, A.J., Kreutter, D.K., et al., 1996. Spontaneous diabetes mellitus in transgenic mice expressing human islet amyloid polypeptide. Proceedings of the National Academy of Sciences. https://doi.org/10.1073/pnas.93.14.7283.

[25] Höppener, J.W.M., Jacobs, H.M., Wierup, N., Sotthewes, G., Sprong, M., de Vos, P., et al., 2008. Human islet amyloid polypeptide transgenic mice: in vivo and ex vivo models for the role of hIAPP in type 2 diabetes mellitus. Experimental Diabetes Research 697035. https://doi.org/10.1155/2008/697035.

[26] Wicksteed, B., Brissova, M., Yan, W., Opland, D.M., Plank, J.L., Reinert, R.B., et al., 2010. Analysis of ectopic cre transgene expression in the brain. Diabetes 1(18):3090–3098. https://doi.org/10.2337/db10-0624.

[27] Paulsson, J.F., Westermark, G.T., 2005. Aberrant processing of human proislet amyloid polypeptide results in increased amyloid formation. Diabetes. https://doi.org/10.2337/diabetes.54.7.2117.

[28] Schmidt, V., Sporbert, A., Rohe, M., Reimer, T., Rehm, A., Andersen, O.M., et al., 2007. SorLA/LR11 regulates processing of amyloid precursor protein via interaction with adaptors GGA and PACS-1. Journal of Biological Chemistry 282(45):32956–32964. https://doi.org/10.1074/jbc.M705073200.

[29] Wu, C., Shea, J.-E., 2013. Structural similarities and differences between amyloidogenic and non-amyloidogenic islet amyloid polypeptide (IAPP) sequences and implications for the dual physiological and pathological activities of these peptides. PLoS Computational Biology 9(8):e1003211. https://doi.org/10.1371/journal.pcbi.1003211.

[30] Kitago, Y., Nagae, M., Nakata, Z., Yagi-Utsumi, M., Takagi-Niidome, S., Mihara, E., et al., 2015. Structural basis for amyloidogenic peptide recognition by sorLA. Nature Structural & Molecular Biology 22(3):199–206. https://doi.org/10.1038/nsmb.2954.

[31] Clark, A., Saad, M.F., Nezzer, T., Uren, C., Knowler, W.C., Bennett, P.H., et al., 1990. Islet amyloid polypeptide in diabetic and non-diabetic Pima Indians. Diabetologia 33(5):285–289. https://doi.org/10.1007/BF00403322.

[32] Westermark, G., Arora, M.B., Fox, N., Carroll, R., Chan, S.J., Westermark, P., et al., 1995. amyloid formation in response to β cell stress occurs in vitro, but not in vivo, in islets of transgenic mice expressing human islet amyloid polypeptide. Molecular Medicine 1(5):542–553. https://doi.org/10.1007/BF03401591.

[33] Wang, J., Xu, J., Finnerty, J., Furuta, M., Steiner, D.F., Verchere, C.B., 2001. The prohormone convertase enzyme 2 (PC2) is essential for processing pro-islet amyloid polypeptide at the NH2-terminal cleavage site. Diabetes 50(3):534–539. https://doi.org/10.2337/diabetes.50.3.534.

[34] Marzban, L., Trigo-Gonzalez, G., Zhu, X., Rhodes, C.J., Halban, P.A., Steiner, D.F., et al., 2004. Role of β-cell prohormone convertase (PC)1/3 in processing of pro-islet amyloid polypeptide. Diabetes 53(1):141–148. https://doi.org/10.2337/diabetes.53.1.141.

[35] Chen, Y.C., Mains, R.E., Eipper, B.A., Hoffman, B.G., Czyzyk, T.A., Pintar, J.E., et al., 2020. PAM haploinsufficiency does not accelerate the development of diet- and human IAPP-induced diabetes in mice. Diabetologia 63(3):561–576. https://doi.org/10.1007/s00125-019-05060-z.

[36] Marzban, L., Soukhatcheva, G., Verchere, C.B., 2005. Role of carboxypeptidase E in processing of pro-islet amyloid polypeptide in β-cells. Endocrinology 146(4):1808–1817. https://doi.org/10.1210/en.2004-1175.

[37] Cool, D.R., Loh, Y.P., 1998. Carboxypeptidase E is a sorting receptor for prohormones: binding and kinetic studies. Molecular and Cellular Endocrinology 139(1–2):7–13. https://doi.org/10.1016/S0303-7207(98)00081-1.

[38] Irminger, J.C., Verchere, C.B., Meyer, K., Halban, P.A., 1997. Proinsulin targeting to the regulated pathway is not impaired in carboxypeptidase E-deficient Cpe(fat)/Cpe(fat) mice. Journal of Biological Chemistry 272(44):27532–27534. https://doi.org/10.1074/jbc.272.44.27532.

[39] Malik, A.R., Willnow, T.E., 2020. VPS10P domain receptors: sorting out brain health and disease. Trends in Neurosciences, 1–16. https://doi.org/10.1016/j.tins.2020.08.003.

[40] Kebede, M.A., Oler, A.T., Gregg, T., Balloon, A.J., Johnson, A., Mitok, K., et al., 2014. SORCS1 is necessary for normal insulin secretory granule biogenesis in metabolically stressed β cells. Journal of Clinical Investigation 124(10):4240–4256. https://doi.org/10.1172/JCI74072.

[41] Clee, S.M., Yandell, B.S., Schueler, K.M., Rabaglia, M.E., Richards, O.C., Raines, S.M., et al., 2006. Positional cloning of Sorcs1, a type 2 diabetes quantitative trait locus. Nature Genetics 38(6):688–693. https://doi.org/10.1038/ng1796.

[42] Goodarzi, M.O., Lehman, D.M., Taylor, K.D., Guo, X., Cui, J., Quiñones, M.J., et al., 2007. SORCS1: a novel human type 2 diabetes susceptibility gene suggested by the mouse. Diabetes 56(7):1922–1929. https://doi.org/10.2337/db06-1677.

[43] Quistgaard, E.M., Madsen, P., Grøftehauge, M.K., Nissen, P., Petersen, C.M., Thirup, S.S., 2009. Ligands bind to Sortilin in the tunnel of a ten-bladed β-propeller domain. Nature Structural & Molecular Biology 16(1):96–98. https://doi.org/10.1038/nsmb.1543.

[44] Marzban, L., Rhodes, C.J., Steiner, D.F., Haataja, L., Halban, P.A., Verchere, C.B., 2006. Impaired NH2-terminal processing of human proislet amyloid polypeptide by the prohormone convertase PC2 leads to amyloid formation and cell death. Diabetes. https://doi.org/10.2337/db05-1566.

[45] Akter, R., Cao, P., Noor, H., Ridgway, Z., Tu, L.H., Wang, H., et al., 2016. Islet amyloid polypeptide: structure, function, and pathophysiology. Journal of Diabetes Research. https://doi.org/10.1155/2016/2798269.

[46] Aston-Mourney, K., Hull, R.L., Zraika, S., Udayasankar, J., Subramanian, S.L., Kahn, S.E., 2011. Exendin-4 increases islet amyloid deposition but offsets the resultant beta cell toxicity in human islet amyloid polypeptide transgenic mouse islets. Diabetologia 54(7):1756–1765. https://doi.org/10.1007/s00125-011-2143-3.

[47] Gurlo, T., Ryazantsev, S., Huang, C.J., Yeh, M.W., Reber, H.A., Hines, O.J., et al., 2010. Evidence for proteotoxicity in β cells in type 2 diabetes: toxic islet amyloid polypeptide oligomers form intracellularly in the secretory pathway. American Journal Of Pathology 176(2):861–869. https://doi.org/10.2353/ajpath.2010.090532.

[48] Westermark, P., Engstrom, U., Johnson, K.H., Westermark, G.T., Betsholtz, C., 1990. Islet amyloid polypeptide: pinpointing amino acid residues linked to amyloid fibril formation. Proceedings of the National Academy of Sciences of the United States of America 87(13):5036–5040. https://doi.org/10.1073/pnas.87.13.5036.

[49] Höppener, J.W.M., Oosterwijk, C., Nieuwenhuis, M.G., Posthuma, G., Thijssen, J.H.H., Vroom, T.M., et al., 1999. Extensive islet amyloid formation is induced by development of Type II diabetes mellitus and contributes to its progression: pathogenesis of diabetes in a mouse model. Diabetologia 42(4):427–434. https://doi.org/10.1007/s001250051175.

[50] Hull, R.L., Andrikopoulos, S., Verchere, C.B., Vidal, J., Wang, F., Cnop, M., et al., 2003. Increased dietary fat promotes islet amyloid formation and β-cell secretory dysfunction in a transgenic mouse model of islet amyloid. Diabetes 52(2):372–379. https://doi.org/10.2337/diabetes.52.2.372.

[51] MacArthur, D.L.A., De Koning, E.J.P., Verbeek, J.S., Morris, J.F., Clark, A., 1999. Amyloid fibril formation is progressive and correlates with beta-cell secretion in transgenic mouse isolated islets. Diabetologia 42(10):1219–1227. https://doi.org/10.1007/s001250051295.

[52] Jurgens, C.A., Toukatly, M.N., Fligner, C.L., Udayasankar, J., Subramanian, S.L., Zraika, S., et al., 2011. β-Cell loss and β-cell apoptosis in human type 2 diabetes are related to islet amyloid deposition. American Journal Of Pathology. https://doi.org/10.1016/j.ajpath.2011.02.036.

[53] Lorenzo, A., Razzaboni, B., Weir, G.C., Yankner, B.A., 1994. Pancreatic islet cell toxicity of amylin associated with type-2 diabetes mellitus. Nature 368(6473):756–760. https://doi.org/10.1038/368756a0.

[54] Potter, K.J., Scrocchi, L.A., Warnock, G.L., Ao, Z., Younker, M.A., Rosenberg, L., et al., 2009. Amyloid inhibitors enhance survival of cultured human islets. Biochimica et Biophysica Acta (BBA) - General Subjects 1790(6):566–574. https://doi.org/10.1016/j.bbagen.2009.02.013.

